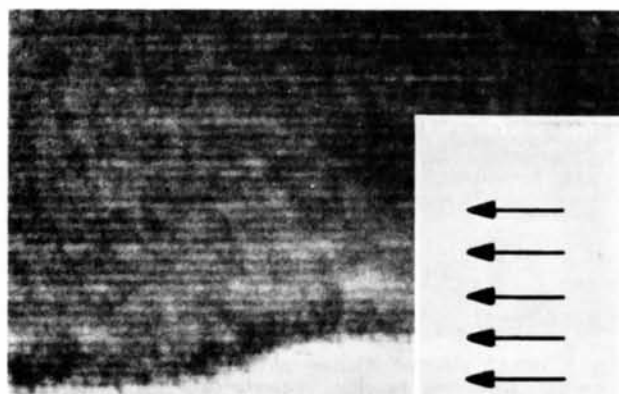


Fig. 1. Scanning electron micrograph of a typical single-crystal lath, showing stepwise changes in thickness parallel to the long edge. The region enclosed by a black line is shown at higher magnification in the inset, indicating a 250 Å edge thickness.



(a)



(b)

Fig. 2. 100 kV transmission micrographs from an edge region similar to that shown in Fig. 1. In (a) the objective stigmator has been adjusted so that some asymmetry remains parallel to the lattice fringes, thereby enhancing the signal-to-noise ratio. The inset shows a projected charge-density calculation, made for a vacancy-plane structure according to a model with screened  $K^+$  ions occupying the hexagonal tunnel of the structure. The thin-crystal region of 200–300 Å extends only about 100 Å in from the edge, which occurs at a potential vacancy plane. (b) Shows an edge region including a surface step, illustrating the tendency of the crystal to terminate on superlattice planes (superlattice spacing is indicated by arrows).

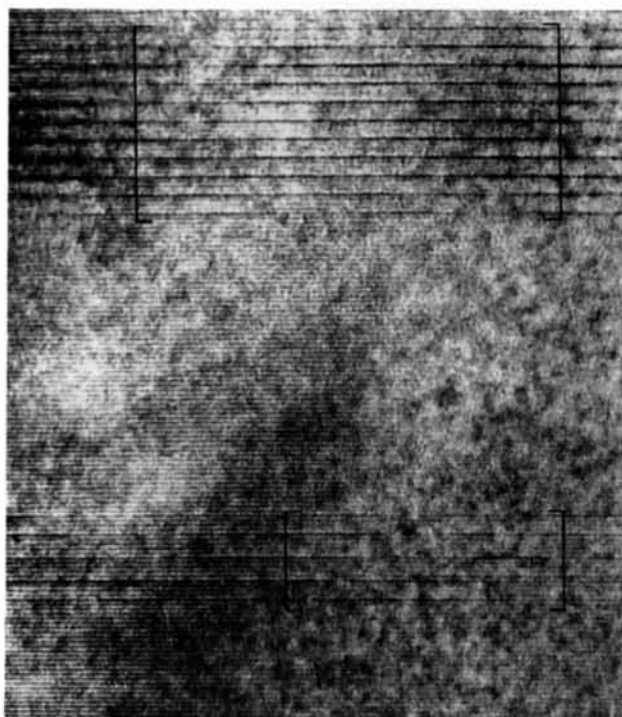


Fig. 3. 100 kV electron micrograph from a partially oxidized crystal. Black-line brackets indicate two regions of independent nucleation of the superlattice. The two regions are mutually out of phase.

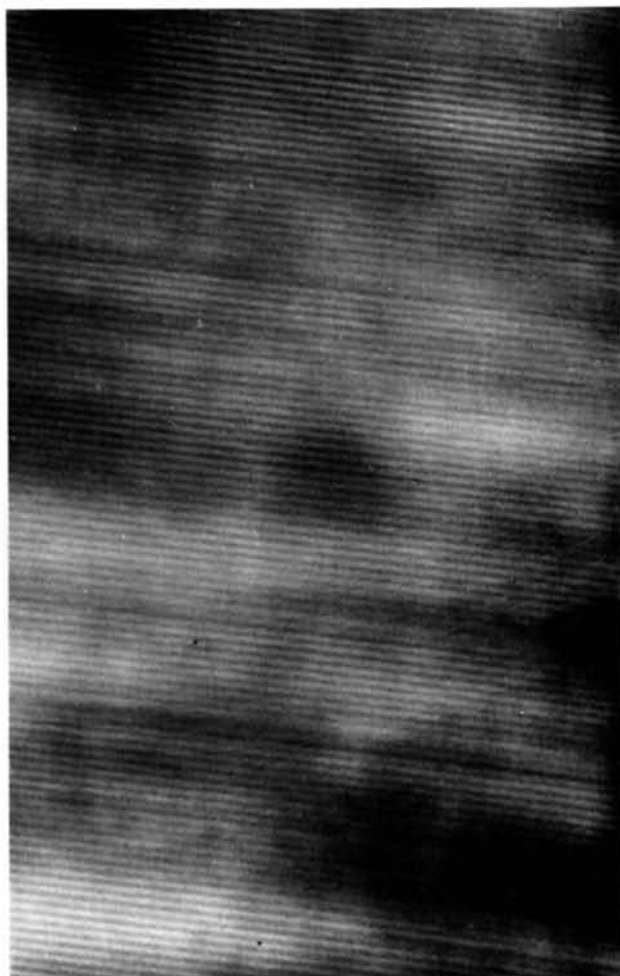


Fig. 4. An out-of-focus micrograph showing only the superlattice with 26 Å spacing from an oxidized tungsten-bronze crystal. The superlattice is coherent throughout this region; however, a local variation in contrast indicates a variation in the occupation density of the superlattice planes which is generally slight but locally quite marked.

subcell dimensions appreciably, it is suggested that model 2, with  $K^+$  ions electrostatically bonded to the host lattice, is the most probable. In this model, as oxidation proceeds some of the negative lattice charge is captured by O atoms, which then occupy sites without radically changing the electrostatic environment.

Finally, a brief study was made of the original black, and reduced, tungsten bronze to see if any type of ordering could be detected by electron diffraction, other than the doubling of the  $c$  axis reported originally by Magnéli & Blomberg (1951). Samples of this material were ground and examined by selected-area diffraction. Most of the crystals examined had the hexagonal structure. The patterns from these showed no measurable diffuse scattering but a twofold superlattice was recorded in upper layer lines from at least some of the crystals. However, no extra reflexions were visible in the zero layer of [001] projection. It is therefore feasible that the twofold  $c$  axis is the same as reported by Magnéli & Blomberg, and that it is associated with a doubling of the  $a$  axis; this doubling may be very difficult to detect by X-ray diffraction. The observed superlattice shown in Fig. 7 is different in character from the one described here for the oxidized structure, since the latter has a strong contribution in the  $h00$  line.

### 7. Conclusions

From this study we conclude that: (a) superlattice formation occurs in the oxidized tungsten bronze as a

result of two almost independent processes; (b) oxidation (and reduction) occurs continuously without appreciable dimensional disturbance of the host lattice.

In conclusion, it would be of interest to investigate the reduced bronze more thoroughly, and to examine consequences of the evident mobility of O in the structure.

The author wishes to thank Mr Frank Bailey for continuous cooperation in operating the high-temperature furnaces, and Professor Kihlborg for helpful discussions and criticism. In addition, the cooperation of Monash University Chemistry Department, and Dr Bryan Gatehouse in particular, in providing samples of tungsten bronze made by solid-state reaction, is gratefully acknowledged.

### References

- BURSILL, L. A. & HYDE, B. G. (1972). *Nature Phys. Sci.* **240**, 122–124.  
 DENNE, W. A. & GOODMAN, P. (1973). *Acta Cryst.* **B29**, 2314–2315.  
 DESCHANVRES, G., DESGARDIN, G., RAVEAU, B. & THOMAZEAU, J. C. (1967). *Bull. Soc. Chim. Fr.* **12**, 4537–4541.  
 GOODMAN, P. & MCLEAN, J. D. (1976). *Acta Cryst.* **B32**, 3285–3286.  
 MAGNÉLI, A. & BLOMBERG, B. (1951). *Acta Chem. Scand.* **5**, 372–378.

*Acta Cryst.* (1976). **B32**, 3285

## Direct Imaging of Ordering in $K_xWO_{(3+y)}$

BY P. GOODMAN AND J. D. MCLEAN

*Division of Chemical Physics, CSIRO, P.O. Box 160, Clayton, Victoria, Australia 3168*

(Received 23 January 1976; accepted 15 March 1976)

Lattice images from vapour-grown crystals of  $K_xWO_{(3+y)}$  with  $x \approx 0.27$  and  $y \approx x/2$  show that long-range ordering of 26 Å periodicity perpendicular to the ( $h00$ ) planes is consistent with a two-dimensional ordering of vacancies amongst the  $K^+$  ion sites. The independent nucleation of long-range order in neighbouring crystal regions during the process of oxidation is shown in the micrographs.

Crystals of  $K_xWO_{(3+y)}$  with  $x \approx 0.27$  and  $y \approx x/2$  grown from the vapour phase at above 1300°C give electron diffraction patterns which exhibit two superstructures, one arising from the W and one from the K lattice (Goodman, 1976). The diffraction evidence shows that the  $K^+$  structure has a planar ordering, but the nature of the ordering cannot be definitely established from diffraction evidence alone. For this purpose high-resolution electron micrographs were taken, from the  $h00$  systematic reflexions. The crystals used were taken

directly from the vapour-grown preparation. To assist with the interpretation of the transmission micrographs a series of scanning electron micrographs was taken from crystals typical of the specimens used for transmission study. These micrographs showed approximately plane-parallel lamellae, with discontinuous changes in thickness (Fig. 1). Thin regions frequently occurred along the edges, and these regions were typically 200–300 Å thick.

Fig. 2(a) shows a typical region near an edge, with